Role of miR-195 in Aortic Aneurysmal Disease

Anna Zampetaki[1], Rizwan Attia[1], Ursula Mayr[1], Renata S.M. Gomes[1], Alkystis Phinikaridou[1], Xiaoke Yin[1], Sarah R. Langley[1], Peter Willeit[2], Ruifang Lu[1], Bruce Fanshawe[1], Marika Fava[1,3], Javier Barallobre-Barreiro[1], Chris Molenaar[1], Po-Wah So[4], Abeera Abbas[1], Marjan Jahangiri[3], Matthew Waltham[1], Rene Botnar[1], Alberto Smith[1] and Manuel Mayr[1]

[1]King's British Heart Foundation Centre, King's College London, UK; [2]Department of Public Health and Primary Care, University of Cambridge, UK; [3]Department of Cardiac Surgery, St. George's Healthcare NHS Trust, London, UK, and; [4] Institute of Psychiatry, King's College London, UK.

***Running title*:** MiR-195 and Aortic Aneurysms

Subject codes:
[97] Other Vascular Biology
[115] Remodeling
[141] Functional Genomics

Address correspondence to:

Dr Anna Zampetaki
King's British Heart Foundation Centre
King's College London
125 Coldharbour Lane
London SE59NU
United Kingdom
Tel: +44 (0)20 7848 5132
Fax: +44 (0)20 7848 5296
anna.zampetaki@kcl.ac.uk

Dr. Manuel Mayr
King's British Heart Foundation Centre
King's College London
125 Coldharbour Lane
London SE59NU
United Kingdom
Tel: +44 (0)20 7848 5132
Fax: +44 (0)20 7848 5296
manuel.mayr@kcl.ac.uk

In August, 2014, the average time from submission to first decision for all original research papers submitted to *Circulation Research* was 13.55 days

ABSTRACT

Rationale: Abdominal aortic aneurysms (AAA) constitute a degenerative process in the aortic wall. Both the miR-29 and miR-15 families have been implicated in regulating the vascular extracellular matrix.

Objective: To assess the effect of the miR-15 family on aortic aneurysm development.

Methods and Results: Among the miR-15 family members, miR-195 was differentially expressed in aortas of apolipoprotein E-deficient mice upon angiotensin II infusion. Proteomics analysis of the secretome of murine aortic smooth muscle cells, following miR-195 manipulation, revealed that miR-195 targets a cadre of extracellular matrix proteins, including collagens, proteoglycans, elastin and proteins associated with elastic microfibrils; albeit miR-29b showed a stronger effect, particularly in regulating collagens. Systemic and local administration of cholesterol-conjugated antagomiRs revealed better inhibition of miR-195 compared to miR-29b in the uninjured aorta. However, in apolipoprotein E-deficient mice receiving angiotensin II, silencing of miR-29b, but not miR-195 led to an attenuation of aortic aneurysm formation. Higher aortic elastin expression was accompanied by an increase of matrix metalloproteinases 2 and 9 in mice treated with antagomiR-195. In human plasma, an inverse correlation of miR-195 was observed with the presence of AAA and aortic diameter.

Conclusions: We provide the first evidence that miR-195 may contribute to the pathogenesis of aortic aneurysmal disease. Although inhibition of miR-29b proved more effective in preventing aneurysm formation in a preclinical model, miR-195 represents a potent regulator of the aortic extracellular matrix. Notably, plasma levels of miR-195 were reduced in patients with AAA suggesting that miRNAs might serve as a noninvasive biomarker of AAA.

Keywords:
microRNA, aneurysm, extracellular matrix, smooth muscle cell, biomarker

Nonstandard Abbreviations and Acronyms:

AAA	Abdominal aortic aneurysm
Ang II	Angiotensin II
ECM	Extracellular matrix
SMC	Aortic smooth muscle cells
MiRNA	MicroRNA
MMP	Matrix metalloproteinases
NSAF	Normalized spectral abundance factor

INTRODUCTION

MicroRNAs (miRNAs) are small non-coding RNAs that are involved in posttranscriptional regulation of gene expression[1, 2]. Recent studies have uncovered pronounced effects of miRNAs on the cardiovascular extracellular matrix (ECM). The miR-29 family has attracted particular attention. It consists of three members that exhibit very high homology, miR-29a, miR-29b and miR-29c. In the heart, dysregulation of miR-29b coincided with ECM remodeling after acute myocardial infarction[3]. In the vasculature, inhibition of miR-29 has been consistently shown to reduce aortic aneurysm formation[4-6]. Although there is conflicting evidence for the directionality of the changes of miR-29b expression in angiotensin II (Ang II)-induced murine aneurysms, targeting of elastin and collagens was proposed as the underlying mechanism for the role of miR-29b in aneurysmal disease[4-7].

The ECM is the key structural component determining dilatation and aneurysm formation in the aortic wall[8]. Abdominal aortic aneurysms (AAA) are characterized by loss of elastin and increased collagen turnover. Apart from miR-29, the miR-15 family has been implicated in collagen remodeling and the characteristic postnatal silencing of elastin[9]. The miR-15 family consists of six highly conserved miRNAs (miR-15a, miR-15b, miR-16-1, miR-16-2, miR-195 and miR-497), which are clustered on 3 separate chromosomes. They have a common seed region (AGCAGCA) and varying degrees of sequence homology in the 3' region of the mature miRNA[10]. Expression of miR-195 and miR-497 is altered in human aortic specimen with evidence of dissection[11]. Direct binding of miR-195 to several ECM transcripts was detected in H4 cancer cells[12].

In the present study, we compare the role of miR-29 and miR-15 family members in aortic aneurysm development. Besides biomarker candidates, the regulation of the vascular ECM by miRNAs may reveal novel mechanistic insights and potential therapeutic targets.

METHODS

An expanded Materials and Methods section is available in the Online Data Supplement.

Clinical cohorts.
Patients with AAA were identified from the local aneurysm surveillance and screening programme. Subjects screened negative for AAA served as controls. The study was approved by the local research ethics committee and all patients provided written informed consent (REC 07/Q0702/62). Statistical analysis was performed as described previously[13].

Cell culture.
Smooth muscle cells (SMCs) were isolated by enzymatic digestion of mouse aortas, as described elsewhere[14] and were cultured in DMEM supplemented with 10% FCS, 2 mmol/L L-glutamine and 100 mg/L gentamicin, at 37ºC in a humidified atmosphere of 95% air / 5% CO_2.

Transfections.
Cells were plated at 60-70% confluency on the day before transfection. Mouse Pre-miR™ miRNA precursors and miRNA mimics were synthesized by Life Technologies and Mercury™ LNA-anti-miRs by Exiqon. The following sequences were used: LNA-195: CCAATATTTCTGTGCTGCT; LNA-29b: ACTGATTTCAAATGGRGCT; LNA-CTL: GTGTAACACGTCTATACGCCCA; Pre-miR-195:UAGCAGCACAGAAAUAUUGGC; Pre-miR-29b: UAGCACCAUUUGAAAUCAGUGUU; Pre-miR-CTL2: sequence not specified. LNA inhibitors and precursor miRNA were transfected at a final

concentration of 90 nmol/L and 20nmol/L respectively, using Lipofectamine™ RMAiMAX (Invitrogen) according to the manufacturer's recommendations.

Proteomics analysis.
SMCs were carefully washed in serum-free medium and then incubated in fresh serum free medium for 48 hours. Cell debris was removed by centrifugation at 4000 rpm for 10 min. The supernatant was transferred into a new tube and stored at -80°C. Samples were subsequently desalted using Zeba Spin desalting columns (Thermo Scientific), vacuum dried and resuspended in 60 µL of ddH_2O. 30 µL was used for the proteomic analysis as described previously[15].

AntagomiR treatment.
Cholesterol-conjugated antagomiR constructs from Fidelity Biosystems were resuspended in sterile PBS at 37°C and stored at -20°C. The sequences of the antagomiR constructs were as follows:

Control AntagomiR: 5`- A*A*GGCAAGCUGACCCUGAA*G*U*U* Chol*T-3'
AntagomiR-195: 5`- G*C*CAAUAUUUCUGUGCU*G*C*U* Chol*T-3'
AntagomiR-29b: A*A*CACUGAUUUCAAAUGGUG*C*U*A*-Chol*T-3'

C57BL6 mice were treated by intraperitoneal (i.p.) injection with a dose of 65 mg/kg/day at day 0, day 1 and day 2. Mice were sacrificed at day 7 to collect aortic tissue.

Angiotensin II infusion model.
Osmotic pumps (Alzet model 2004) containing angiotensin II (Ang II, 1 µg/kg/min, Sigma-Aldrich) were implanted in 10-week-old *apoE-/-* male mice (day 0) (C57BL/6J background, Charles River Edinburgh UK). Housing and animal care was in accordance with the UK Animals (Scientific Procedures) Act 1986. The antagomiR constructs were injected i.p. at a dose of 80 mg/kg/day on three consecutive days (day 1, 2 and 3).

MRI imaging.
Mice were imaged by MRI before and after implantation of osmotic pumps to obtain aortic and cardiac parameters. The aortic scans were performed using 0.4mmol/kg of an elastin-specific magnetic resonance agent[16, 17].

RESULTS

MiR-195 in murine aortas.

Elastin is the major structural protein that imparts elasticity to blood vessels. Degradation of elastin is an early event in the development of aortic aneurysms. Two miRNA families, miR-29 and miR-15, have been linked to elastin regulation. Differential expression of miR-29b in the aneurysmal aorta has been reported previously[4, 5]. Here, we investigated the expression of miR-15 family members in a mouse model of aortic dilation. Ang II (1µg/kg/min) was infused to *apoE-/-* mice using subcutaneously implanted osmotic minipumps. Among the miR-15 family, only miR-195 was significantly increased (Online Figure I). The miRWALK algorithm predicts putative binding sites for miR-195 and miR-29b in the coding region and the 3'UTR of elastin, respectively. Overexpression of miR-195 as well as miR-29b led to a similar reduction in elastin (Online Figure II). Reporter assays using vectors harboring these sites revealed reduced activity, suggesting that elastin is a direct target of both miRNAs. While miR-29b has been investigated previously[4-6], little is known about the role of miR-195 in the vasculature.

MiR-195 and ECM secretion by SMCs.

To further explore the effect of miR-195 on ECM deposition by SMCs, we performed a proteomic analysis of the conditioned medium from SMCs transfected with pre-miRs and anti-miRs. A total of 129 secreted proteins were identified, with pre-miRs having a more pronounced effect than anti-miRs (Figure 1, Online Table I and II). A normalized spectral abundance factor normalization coupled with a power law global error model (NSAF-PLGEM) was employed to determine the differences in expression. Proteins with a false discovery rate <5% were considered to be significant. Transfection with pre-miR-195 induced differential expression of 87 proteins in the secretome of SMCs. Using different miRNA prediction algorithms (RNA22, miRanda, miRDB, TargetScan, RNAhybrid, PITA, PICTAR and Diana-microT), only 24 of them were predicted as direct targets.

Comparison with miR-29b.

30 ECM genes and ECM degrading enzymes were quantified in SMCs following transfection with inhibitors and mimics of miR-195 and miR-29b. As expected, both miR-29b and miR-195 targeted elastin (Eln, Figure 2A). However, the gene expression profiles of extracellular proteins differed. For example, mimics of miR-29b elicited a more robust repression of collagens (col1a1, col1a2, col3a1, col4a1, col4a2, col5a1, col5a2). These results were also validated at the protein level by immunoblotting (Figure 2B). Notably, matrix metalloproteinase (MMP) 2 expression was increased upon miR-195 inhibition, while targeting miR-29b led to a reduction of MMP9 (Figure 2C) as confirmed by zymography (Figure 2D, Online Figure IID).

Systemic inhibition of miR-195 and miR-29b.

To determine the role of miR-29b and miR-195 in ECM gene regulation in vivo, C57Bl wild type mice were injected with cholesterol-conjugated antagomiRs (65mg/kg/day, i.p.). AntagomiR-195 was effective in targeting miR-195 expression in the aorta leading to a 60% reduction without affecting other members of the miR-15 family (Figure 3A). Similarly, no off-target effect on the miR-29 family was observed (compared to control antagomiR: 1.17±0.12, 1.13±0.13 and 1.11±0.09 for miR-29a, miR-29b and miR-29c, respectively. N=5 per group). In vivo inhibition of miR-195 increased expression of elastin (Figure 3B) and of several other ECM genes in the aorta (Figure 3C, Online Figure III). Detailed expression data are presented in Online Figure IV. Surprisingly, the same dose of antagomiR-29b had only marginal effects on miR-29b levels in the uninjured aorta. The observed reduction of miR-29b in the vasculature was small (Figure 3D), and aortic elastin expression was not affected (Figure 3E). A negative correlation between miR-29b levels and ECM genes in the aorta was observed for Col1a1, Col1a2, Col4a2 (Figure 3F) and few other targets (Online Figure V). Detailed expression data are presented in Online Figure VI. In contrast, a marked suppression of miR-29b was observed in the liver. Accordingly, elastin and other ECM genes were upregulated in the liver of mice injected with antagomiR-29b (Online Figure VII). Thus, the uninjured aorta is more susceptive for therapeutic interventions by antagomiR-195 than antagomiR-29b.

Effect of miR-195 and miR-29b on aortic aneurysm formation.

To study whether miR-195 may contribute to the pathogenesis of AAA, we compared the effects of miR-195 and miR-29b inhibition on aneurysm formation. AntagomiRs were administered systemically as detailed in the Methods. Uptake of a Cy3 labeled antagomiR was detected in the medial layer of the murine aorta (Online Figure VIII). The total aortic wall area was determined by using an elastin-specific magnetic resonance contrast agent[18] (Figure 4A). A significant decrease in the aortic diameter size was observed in mice treated with antagomiR-29b (n=8, Figure 4B). This was accompanied by enhanced survival compared to control antagomiR and PBS injected mice (n=8 each, Figure 4C). Despite significantly elevated expression of elastin and collagens (Online Figure IX), the effect of antagomiR-195 on survival as well as aortic diameter size was not as pronounced (Figure 4B and 4C).

Local inhibition of miR-195 and miR-29b in aortic isografts.

To discern systemic from local effects, we used an aortic isograft model[19]. Aortas were harvested, incubated with cholesterol bound LNA antimiRs for 2 hours and then isografted into the carotid artery of recipient mice (Figure 5A). This local administration was sufficient to result in an uptake of the antagomiRs by the aortic tissue, as demonstrated by the incorporation of a Cy3 labelled antagomiR in the outer layers of SMCs (Figure 5B). The grafts were harvested 7 days later and expression levels of miRNAs were determined. In this setting, miR-195 was significantly inhibited, while other members of the miR-15 family were largely unaffected (Figure 5C). Local inhibition of miR-195 was accompanied by derepression of MMPs, in particular MMP2, in the aortic wall (Figure 5D). The same dose of LNA-miR-29b did not significantly inhibit miR-29 expression in aortic grafts (data not shown). In vivo inhibition of miR-195 resulted in a derepression of MMPs in all three models (Figure 5E), including aortic tissue of Ang II infused *apoE-/-* mice (Online Figure X).

MiR-195 in patients with aortic aneurysms.

Finally, plasma samples were obtained from the local aneurysm surveillance and screening programme designed to identify patients with abdominal aortic aneurysms (AAAs). Male patients with AAAs and male controls were matched on hypertension and diabetes (Table 1). Fifteen other miRNAs, including some previously related to cardiovascular disease, were added for comparison. Statistical analyses were performed using conventional and L_1-penalized logistic/linear regression, with the latter being developed to explore associations in presence of high-dimensional and collinear data. MiR-195 showed the strongest associations using either a continuous (aortic diameter size, n=44, Figure 6) or a categorical classification of disease (n=22 per group, Figure 7). Other miRNAs displaying significant inverse correlations with aortic diameter size included miR-148a, miR- 125b, miR-20a and miR-340. Expression levels of these four miRNAs, however, were highly correlated to miR-195 (Online Table III) and their association with aortic diameter size was attenuated after adjustment for miR-195 (Online Figure XI and XII). Instead, significant associations emerged for miR-133a and miR-145, suggesting that their relation to AAA may be independent of miR-195. The significant inverse associations of miR-195 with the presence of AAA and the aortic diameter was confirmed by extending the analyses to all participants in the programme (n=73, Online Table IV, Online Figure XIII and XIV). In comparison to miR-195, miR-29b levels in plasma were low (Ct>32 cycles, Online Figure XV) rendering plasma miR-29b less suitable as a biomarker of AAA.

DISCUSSION

The principal merits of this study are i) the measurements of plasma miRNAs in a patient cohort of AAA and ii) the direct comparison of two miRNA families known to target elastin in in vitro studies in vascular SMCs and in in vivo studies using three different animal models (uninjured aorta and aortic isografts in wildtype mice, Ang II infusion in *apoE-/-* mice). Although both miR-195 and miR-29b affect elastin in vitro and antagomiRs to miR-195 were more efficient in upregulating aortic elastin expression in vivo, antagomiR treatment to miR-195 did not recapitulate the protective effects of miR-29b inhibition on aneurysm formation. In contrast to miR-29b, silencing of miR-195 induced a de-repression of MMPs, which is likely to contribute to the adverse outcome in ECM homeostasis. MiR-195, however, emerged as a biomarker candidate for AAA.

MiRNAs as biomarkers.

We have previously performed the first population-based study on circulating miRNAs for type II diabetes[20] and myocardial infarction[13]. We also determined the platelet origin of several plasma miRNAs

related to cardiovascular disease by subjecting healthy volunteers to limb ischemia-reperfusion injury generated by thigh cuff inflation[13] and performing a dose-escalation study of platelet inhibition[21]. The association of plasma miRNAs and AAA is unclear. In the present study, we measured 16 miRNAs in 73 participants from a local aneurysm surveillance and screening programme. Among the most robust changes was miR-195, which dominated the penalized regression analyses for aortic diameter size and categorical disease outcome in terms of association strength. MiR-195 belongs to the miR-15 family that consists of highly conserved miRNAs that regulate key processes in cancer, neural and cardiovascular diseases. MiR-195 expression increases in cardiac hypertrophy, and cardiac overexpression of miR-195 resulted in heart failure in transgenic mice[22]. To our knowledge this is the first report associating plasma levels of miR-195 with aortic disease.

Clinical relevance.

Aortic disease leads to significant morbidity and mortality as well as high economic burden[23, 24]. There are currently no good blood tests that identify patients with AAA or predict which AAAs are likely to rupture or expand and require surgical intervention. The diameter of the aneurysm is currently the best predictor of rupture but not always reliable. Better diagnostic tools are urgently needed to identify patients at risk, monitor disease progression, and implement novel therapeutic and preemptive strategies[25-27]. Identification of those patients with AAAs at risk of subsequent expansion or rupture by a simple cheap non-invasive method of predicting subsequent AAA growth would meet an important clinical need. Once AAA is diagnosed, patients at high risk may be treated with earlier surgical repair to prevent rupture. Conversely, if a simple blood test showed a low risk of disease progression then patients with significant co-morbidity or high surgical risk might be safely kept under surveillance rather than proceed with surgery. Our findings await confirmation in larger cohorts. Thus, their exploratory/hypothesis-generating nature has to be emphasized. Future studies will need to show whether AAA-specific miRNA profiles that characterize aneurysm formation and/or positive responders to treatment might lead to the development of innovative miRNA-based diagnostic and therapeutic strategies for AAA.

MiRNAs and AAA.

Thus far, miR-29b was identified as a pivotal regulator of aortic dilation in an elastase infusion model of experimental AAA in wildtype mice and in an Ang II infusion model in *apoE*-/- mice[4]. Additionally, miR-21 was implicated as a modulator of proliferation and apoptosis of vascular SMCs during development of AAA[28]. The age-related increase of miR-29 expression was proposed to render the aorta susceptible to aneurysm development, while inhibition of miR-29b, by treatment with LNA-antimiR-29b, reduced aortic dilation after Ang II infusion in aged mice[5]. Similar results were obtained in a model of genetically induced aneurysms in Fibulin-$4^{R/R}$ mice. In Marfan syndrome, a connective tissue disorder that can lead to the development of aortic root aneurysms, expression of miR-29b was increased in the ascending aorta. Inhibition of miR-29b prevented early aneurysm development[6]. Thus, several studies suggest a role for miR-29b in aortic aneurysms. Mechanistically, upregulation of elastin[5], increased collagen deposition[4], and suppression of MMP activity were implicated in reducing aortic dilation following miR-29b inhibition[4].

MiRNA target identification.

Herein, we assess the effect of two elastin-targeting miRNAs, miR-195 and miR-29b, both in vitro and in vivo. We have previously used proteomics to study the role of miR-29b in cardiac fibrosis[15]. We now employ proteomic analysis to characterize the secretome of SMCs following manipulation of miR-195 and perform a comparison of the ECM changes induced by miR-195 and miR-29b. Detailed in vitro analyses showed that miR-195 and miR-29b had similar efficiency in targeting elastin. However, miR-29b exerted a more robust effect on ECM deposition by SMCs than miR-195. Collagens, in particular, are more efficiently targeted by mimics to miR-29b than mimics to miR-195. This is consistent with previous findings by Maegdefessel *et al* showing a significant increase in collagen expression and to a lesser extent

in elastin content upon miR-29 inhibition, although an extensive profiling of ECM genes - as in the present study - was not performed[4].

Targeting efficiency in vivo.

The targets observed in vitro were further confirmed in vivo using cholesterol-conjugated antagomiRs. When the same doses of antagomiRs were administered systemically to C57Bl mice, antagomiRs to miR-195 proved to be more effective in upregulating elastin expression in the uninjured aorta than antagomiRs to miR-29b. In a separate model of Ang II infusion in *apoE*-/- mice, the efficiency of antagomiRs against miR-195 and miR-29b was compared with regards to preventing aneurysm formation, decreasing abdominal aortic diameter and improving survival. AntagomiR-29b was superior to antagomiR-195 in reducing aortic dilation and increasing survival in Ang II-infused *apoE*-/- mice. This therapeutic benefit cannot be solely attributed to the derepression of aortic elastin or collagens: both occurred also following miR-195 inhibition; moreover, targeting of miR-29b in murine aortas was less efficient compared to miR-195, with systemic or local delivery of antagomiRs or antimiRs, respectively.

ECM degradation in AAA.

Considerable evidence from human and experimental animal models of AAA points towards a prominent role for MMP2 and MMP9 in AAA development. Elevated levels of MMP2 and MMP9 activity were reported in the aneurysmal part of the mouse aorta following Ang II infusion[29]. MMP2 and MMP9 are two key proteases in ECM destruction, with MMP2 being unique in its ability to target both elastin and fibrillar collagen[30]. MMP9 on the other hand, is the most abundant gelatinolytic MMP in AAA tissue and is secreted in high levels from AAA explants. MMP9 deficient mice displayed preservation of the elastic lamellae of the aortic wall and were shown to be resistant to aneurysm development[31]. Our observation that miR-195 inhibition induced MMP activity, offers a plausible explanation for the different therapeutic outcome compared to silencing miR-29b.

Conclusion.

In this study, the therapeutic efficacy of miR-195 and miR-29b was compared with regards to regulating ECM and ECM-associated proteins in vitro and in vivo. Additionally, we provide proof-of-principle that miRNAs might have clinical utility as biomarkers for AAA by observing an inverse relationship between plasma miR-195 and the presence of AAA and aortic diameter.

SOURCES OF FUNDING
A. Zampetaki is an Intermediate Fellow of the British Heart Foundation. M. Mayr is a Senior Fellow of the British Heart Foundation. This work was supported by the Fondation Leducq (MIRVAD) and the National Institute of Health Research Biomedical Research Center based at Guy's and St Thomas' National Health Service Foundation Trust and King's College London in partnership with King's College Hospital.

DISCLOSURES
None.

REFERENCES

1. Bartel DP. MicroRNAs: Target recognition and regulatory functions. *Cell*. 2009;136:215-233.
2. Liu N, Olson EN. MicroRNA regulatory networks in cardiovascular development. *Dev Cell*. 2010;18:510-525.
3. van Rooij E, Sutherland LB, Thatcher JE, DiMaio JM, Naseem RH, Marshall WS, Hill JA, Olson EN. Dysregulation of microRNAs after myocardial infarction reveals a role of miR-29 in cardiac fibrosis. *Proc Natl Acad Sci USA*. 2008;105:13027-13032.
4. Maegdefessel L, Azuma J, Toh R, Merk DR, Deng A, Chin JT, Raaz U, Schoelmerich AM, Raiesdana A, Leeper NJ, McConnell MV, Dalman RL, Spin JM, Tsao PS. Inhibition of microRNA-29b reduces murine abdominal aortic aneurysm development. *J Clin Invest*. 2012;122:497-506.
5. Boon RA, Seeger T, Heydt S, Fischer A, Hergenreider E, Horrevoets AJ, Vinciguerra M, Rosenthal N, Sciacca S, Pilato M, van Heijningen P, Essers J, Brandes RP, Zeiher AM, Dimmeler S. MicroRNA-29 in aortic dilation: Implications for aneurysm formation. *Circ Res*. 2011;109:1115-1118.
6. Merk DR, Chin JT, Dake BA, Maegdefessel L, Miller MO, Kimura N, Tsao PS, Iosef C, Berry GJ, Mohr FW, Spin JM, Alvira CM, Robbins RC, Fischbein MP. Mir-29b participates in early aneurysm development in marfan syndrome. *Circ Res*. 2012;110:312-324.
7. Zhang P, Huang A, Ferruzzi J, Mecham RP, Starcher BC, Tellides G, Humphrey JD, Giordano FJ, Niklason LE, Sessa WC. Inhibition of microrna-29 enhances elastin levels in cells haploinsufficient for elastin and in bioengineered vessels--brief report. *Arterioscler Thromb Vasc Biol*. 2012;32:756-759.
8. Daugherty A, Cassis LA. Mechanisms of abdominal aortic aneurysm formation. *Curr Atheroscler Rep*. 2002;4:222-227.
9. Ott CE, Grunhagen J, Jager M, Horbelt D, Schwill S, Kallenbach K, Guo G, Manke T, Knaus P, Mundlos S, Robinson PN. Micrornas differentially expressed in postnatal aortic development downregulate elastin via 3' UTR and coding-sequence binding sites. *PloS One*. 2011;6:e16250.
10. Porrello ER, Johnson BA, Aurora AB, Simpson E, Nam YJ, Matkovich SJ, Dorn GW, 2nd, van Rooij E, Olson EN. Mir-15 family regulates postnatal mitotic arrest of cardiomyocytes. *Circ Res*. 2011;109:670-679.
11. Liao M, Zou S, Weng J, Hou L, Yang L, Zhao Z, Bao J, Jing Z. A microrna profile comparison between thoracic aortic dissection and normal thoracic aorta indicates the potential role of microRNAs in contributing to thoracic aortic dissection pathogenesis. *J Vasc Surg*. 2011;53:1341-1349.
12. Nelson PT, Wang WX, Mao G, Wilfred BR, Xie K, Jennings MH, Gao Z, Wang X. Specific sequence determinants of mir-15/107 microRNA gene group targets. *Nucleic Acids Res*. 2011;39:8163-8172.
13. Zampetaki A, Willeit P, Tilling L, Drozdov I, Prokopi M, Renard JM, Mayr A, Weger S, Schett G, Shah A, Boulanger CM, Willeit J, Chowienczyk PJ, Kiechl S, Mayr M. Prospective study on circulating microRNAs and risk of myocardial infarction. *J Am Coll Cardiol*. 2012;60:290-299.
14. Zampetaki A, Zhang Z, Hu Y, Xu Q. Biomechanical stress induces IL-6 expression in smooth muscle cells via ras/rac1-p38 MAPK-NF-kappaB signaling pathways. *Am J Physiol Heart Circ Physiol*. 2005;288:H2946-2954.
15. Abonnenc M, Nabeebaccus AA, Mayr U, Barallobre-Barreiro J, Dong X, Cuello F, Sur S, Drozdov I, Langley SR, Lu R, Stathopoulou K, Didangelos A, Yin X, Zimmermann WH, Shah AM, Zampetaki A, Mayr M. Extracellular matrix secretion by cardiac fibroblasts: Role of microRNA-29b and microRNA-30c. *Circ Res*. 2013;113:1138-1147.
16. Makowski MR, Wiethoff AJ, Blume U, Cuello F, Warley A, Jansen CH, Nagel E, Razavi R, Onthank DC, Cesati RR, Marber MS, Schaeffter T, Smith A, Robinson SP, Botnar RM. Assessment of atherosclerotic plaque burden with an elastin-specific magnetic resonance contrast agent. *Nat Med*. 2011;17:383-388.
17. Makowski MR, Preissel A, von Bary C, Warley A, Schachoff S, Keithan A, Cesati RR, Onthank DC, Schwaiger M, Robinson SP, Botnar RM. Three-dimensional imaging of the aortic vessel wall using an elastin-specific magnetic resonance contrast agent. *Invest Rad*. 2012;47:438-444.

18. Botnar RM, Wiethoff AJ, Ebersberger U, Lacerda S, Blume U, Warley A, Jansen CH, Onthank DC, Cesati RR, Razavi R, Marber MS, Hamm B, Schaeffter T, Robinson SP, Makowski MR. In vivo assessment of aortic aneurysm wall integrity using elastin-specific molecular magnetic resonance imaging. *Circ Cardiovasc Imaging*. 2014;7:679-689.
19. Zampetaki A, Zeng L, Margariti A, Xiao Q, Li H, Zhang Z, Pepe AE, Wang G, Habi O, deFalco E, Cockerill G, Mason JC, Hu Y, Xu Q. Histone deacetylase 3 is critical in endothelial survival and atherosclerosis development in response to disturbed flow. *Circulation*. 2010;121:132-142.
20. Zampetaki A, Kiechl S, Drozdov I, Willeit P, Mayr U, Prokopi M, Mayr A, Weger S, Oberhollenzer F, Bonora E, Shah A, Willeit J, Mayr M. Plasma microRNA profiling reveals loss of endothelial miR-126 and other microRNAs in type 2 diabetes. *Circ Res*. 2010;107:810-817.
21. Willeit P, Zampetaki A, Dudek K, Kaudewitz D, King A, Kirkby NS, Crosby-Nwaobi R, Prokopi M, Drozdov I, Langley SR, Sivaprasad S, Markus HS, Mitchell JA, Warner TD, Kiechl S, Mayr M. Circulating microRNAs as novel biomarkers for platelet activation. *Circ Res*. 2013;112:595-600.
22. van Rooij E, Sutherland LB, Liu N, Williams AH, McAnally J, Gerard RD, Richardson JA, Olson EN. A signature pattern of stress-responsive micrornas that can evoke cardiac hypertrophy and heart failure. *Proc Natl Acad Sci USA*. 2006;103:18255-18260.
23. Lederle FA, Wilson SE, Johnson GR, Reinke DB, Littooy FN, Acher CW, Ballard DJ, Messina LM, Gordon IL, Chute EP, Krupski WC, Busuttil SJ, Barone GW, Sparks S, Graham LM, Rapp JH, Makaroun MS, Moneta GL, Cambria RA, Makhoul RG, Eton D, Ansel HJ, Freischlag JA, Bandyk D, Aneurysm D, Management Veterans Affairs Cooperative Study G. Immediate repair compared with surveillance of small abdominal aortic aneurysms. *N Engl J Med*. 2002;346:1437-1444.
24. Golledge J, Muller J, Daugherty A, Norman P. Abdominal aortic aneurysm: Pathogenesis and implications for management. *Arterioscler Thromb Vasc Biol*. 2006;26:2605-2613.
25. Hellenthal FA, Buurman WA, Wodzig WK, Schurink GW. Biomarkers of AAA progression. Part 1: Extracellular matrix degeneration. *Nat Rev Cardiol*. 2009;6:464-474.
26. Hellenthal FA, Buurman WA, Wodzig WK, Schurink GW. Biomarkers of abdominal aortic aneurysm progression. Part 2: Inflammation. *Nat Rev Cardiol*. 2009;6:543-552.
27. Klink A, Hyafil F, Rudd J, Faries P, Fuster V, Mallat Z, Meilhac O, Mulder WJ, Michel JB, Ramirez F, Storm G, Thompson R, Turnbull IC, Egido J, Martin-Ventura JL, Zaragoza C, Letourneur D, Fayad ZA. Diagnostic and therapeutic strategies for small abdominal aortic aneurysms. *Nat Rev Cardiol*. 2011;8:338-347.
28. Maegdefessel L, Azuma J, Toh R, Deng A, Merk DR, Raiesdana A, Leeper NJ, Raaz U, Schoelmerich AM, McConnell MV, Dalman RL, Spin JM, Tsao PS. MicroRNA-21 blocks abdominal aortic aneurysm development and nicotine-augmented expansion. *Sci Transl Med*. 2012;4:122ra122.
29. Deng GG, Martin-McNulty B, Sukovich DA, Freay A, Halks-Miller M, Thinnes T, Loskutoff DJ, Carmeliet P, Dole WP, Wang YX. Urokinase-type plasminogen activator plays a critical role in angiotensin II-induced abdominal aortic aneurysm. *Circ Res.* 2003;92:510-517.
30. Aimes RT, Quigley JP. Matrix metalloproteinase-2 is an interstitial collagenase. Inhibitor-free enzyme catalyzes the cleavage of collagen fibrils and soluble native type I collagen generating the specific 3/4- and 1/4-length fragments. *J Biol Chem*. 1995;270:5872-5876.
31. Pyo R, Lee JK, Shipley JM, Curci JA, Mao D, Ziporin SJ, Ennis TL, Shapiro SD, Senior RM, Thompson RW. Targeted gene disruption of matrix metalloproteinase-9 (gelatinase b) suppresses development of experimental abdominal aortic aneurysms. *J Clin Invest*. 2000;105:1641-1649.

FIGURE LEGENDS

Figure 1. Proteomic analysis of SMC secretome. SMCs were transfected with miR-195 precursor, antimiR-195 or their respective controls and their secretome was analyzed by proteomics. ECM proteins identified in the conditioned media and displaying differential expression are depicted in the volcano plots. **A,** Following miR-195 overexpression and **B**, miR-195 inhibition. Log2 (FC), fold change is calculated using the NSAF normalised spectral counts and averaged for three biological replicates.

Figure 2. Regulation of the ECM by miR-29b and miR-195 in vitro. A, Heat maps illustrate the expression levels of potential ECM targets. A panel of 30 genes of the ECM were assessed by QPCR following miRNA overexpression (left panel) and inhibition (right panel). The highlighted targets were predicted by at least one prediction algorithm (RNA22, miRanda, miRDB, TargetScan, RNAhybrid, PITA, PICTAR, and Diana-microT). **B,** Validation of ECM protein secretion in the conditioned media of transfected SMCs by Western blot analysis. Part of the corresponding silver stained gel is shown as loading control in the lowest panel. **C,** MMP2 and MMP9 expression in SMCs following miRNA inhibition in vitro. Gene expression was normalized to beta-actin. *$p<0.05$ compared to LNA-Control. **D,** Enzymatic activity of gelatinases in the conditioned media of SMCs following miR-29b and miR-195 inhibition, as assessed by zymography. Representative of three independent experiments.

Figure 3. Regulation of the ECM by miR-195 and miR-29b in vivo. A, Expression levels of the miR-15 family in the aorta following antagomiR-195 treatment. **B,** Elastin expression in the aorta following antagomiR-195 administration. **C,** Correlation between the efficiency of miR-195 knockdown and the derepression of collagens as quantified by QPCR. **D,** Expression levels of the miR-29 family in the aorta following antagomiR-29b treatment. **E,** Elastin expression in the aorta following antagomiR-29b injection. **F,** Correlation between the efficiency of miR-29b knockdown and the derepression of collagens in the aorta. MiRNA expression was normalized to U6. Gene expression was normalized to beta-actin. *$p<0.05$ compared to AntagomiR control. RQ, relative quantification.

Figure 4. MiRNA inhibition and Ang II-mediated aortic dilatation. Ang II (1μg/kg/min) was infused to *apoE*-/- mice using subcutaneously implanted osmotic minipumps. AntagomiRs (80mg/kg/day) were injected intraperitoneally for three consecutive days. **A,** Magnetic resonance TOF-angiogram of aortas from *apoE*-/- mice infused with Ang II demonstrating a suprarenal aortic aneurysm. The red line indicates the imaging plane of subsequent performed axial MRI sequences. **B,** In vivo assessment of the aortic aneurysm diameter following antagomiR-29b or antagomiR-195 treatment (n=8, per group) on days 10 and 35. AntagomiR-Control and PBS injected mice are designated as Control group (n=16). *$p<0.05$ compared to Control. **C,** Kaplan Meier survival analysis for Ang II-infused mice following injections of antagomiR-29 or antagomiR-195.

Figure 5. Regulation of MMP2 and MMP9 by miR-195. A, Schematic representation of the aortic isograft model. **B,** Uptake of a Cy3-labelled antagomiR by the mouse aorta. SMA: Smooth muscle actin. **C,** Expression levels of the miR-15 family in the aortic graft following LNA-miR-195 treatment *ex vivo*. **D,** Expression of MMP2 and MMP9 in the aortic grafts following miRNA inhibition, as quantified by QPCR. RQ, relative quantification. # $p<0.05$ (Anova with Bonferroni post hoc tests for differences to LNA-miR-29b). **E,** Correlation between the efficiency of miR-195 knockdown and the derepression of MMP2 and MMP9 as quantified by QPCR. MiRNA expression was normalized to U6. Gene expression was normalized to beta-actin. * $p<0.05$ compared to control (Con).

Figure 6. MiRNAs associated with aortic diameter. A, L1-penalized linear regression analysis (least absolute shrinkage and selection operator method). The graph shows linear regression coefficients of miRNAs (y-axis) for different levels of penalization (the tuning parameter λ1 escalates beyond 20). Variables withstanding shrinkage up to high λ1 values are those most relevant for disease prediction. **B,**

Linear regression adjusted for age, matched on hypertension and diabetes (for details see Table 1 and Methods). Expression levels were normalised to exogenous *cel*-miR-39 spike-in control.

Figure 7. MiRNAs associated with AAA. A, L1-penalized logistic regression analysis (least absolute shrinkage and selection operator method). The graph shows logistic regression coefficients of miRNAs (y-axis) for different levels of penalization (the tuning parameter λ1). Variables withstanding shrinkage up to high λ1 values are those most relevant for disease prediction. **B,** Logistic regression adjusted for age, matched on hypertension and diabetes (for details see Table 1 and Methods). Expression levels were normalised to exogenous *cel*-miR-39 spike-in control.

Table 1. Clinical characteristics of selected cases and controls from the AAA screening programme

Variable	Mean (SD) or n (%)		P value
	Cases n=22	Controls n=22	
Age	70.8 (6.2)	66.7 (1.0)	0.008
Hypertension	16 (73%)	16 (73%)	Matched
Diabetes	4 (18%)	4 (18%)	Matched
Aortic diameter	3.9 (0.8)	2.1 (0.3)	<0.0001
Smoking status			0.072
Current	14 (64%)	17 (77%)	
Ex	1 (5%)	4 (18%)	
Never	7 (32%)	1 (5%)	
HPL	11 (50%)	9 (41%)	0.500
COPD	5 (23%)	1 (5%)	0.218
CAD	9 (41%)	3 (14%)	0.070
PVD	6 (27%)	0 (0%)	0.031
Prior CVA	4 (18%)	0 (0%)	0.125
Prior CABG	2 (9%)	1 (5%)	1.000
Major Surgery	9 (41%)	4 (18%)	0.227
Malignancy	7 (32%)	3 (14%)	0.289
BMI	27.4 (4.9)	26.9 (3.5)	0.653
Antiplatelets	12 (55%)	9 (41%)	0.508
Betablockers	8 (36%)	4 (18%)	0.344
ACE inhibitors	9 (41%)	6 (27%)	0.453
Statins	15 (68%)	11 (50%)	0.219

P values were calculated with the paired t-test (continuous variables) or exact McNemar's test (categorical variables).
HPL denotes hyperlipidemia; COPD, chronic obstructive pulmonary disease; CAD, coronary artery disease; PVD, peripheral vascular disease; CVA, cerebral vascular accident; CABG, coronary artery bypass graft; BMI, body mass index; ACE inhibitor, angiotensin-converting-enzyme inhibitor.

Novelty and Significance

What Is Known?

- mircoRNA29-b levels are reduced and levels of its targets are increased in human abdominal aortic aneurysm tissue samples.
- MicroRNA-29b and microRNA-195 have been shown to suppress expression of elastin and collagens.
- MicroRNA-29b is implicated in early aortic aneurysm development in a mouse model of Marfan syndrome.
- Inhibition of microRNA-29b is shown to increase levels of elastin and collagens and protect against aortic aneurysm development and its expansion in mice.

What New Information Does This Article Contribute?

- Inhibition of microRNA-195 increases the expression of elastin in the murine aorta.
- AntagomiR treatment to miR-195 does not recapitulate the protective effects of miR-29b inhibition on aortic dilatation.
- Unlike miR-29b, silencing of microRNA-195 is associated with a depression of matrix metalloproteinases.
- In humans, plasma levels of microRNA-195 are inversely associated with the aortic diameter and the presence of abdominal aortic aneurysms (AAA).

We assessed the effect of two elastin-targeting miRNAs, miR-195 and miR-29b, both in vitro and in vivo. We found that miR-195 regulates extracellular matrix deposition and that its plasma levels were associated with abdominal aortic aneurysms. There are currently no validated biomarkers to identify patients with AAA or predict which AAAs are likely to rupture or expand and require surgical intervention. The diameter of the aneurysm is currently the best predictor of rupture but not always reliable. Studies in larger cohorts are needed to establish whether plasma miRNA signatures can identify patients with AAA at high risk of expansion or rupture.

Figure 1

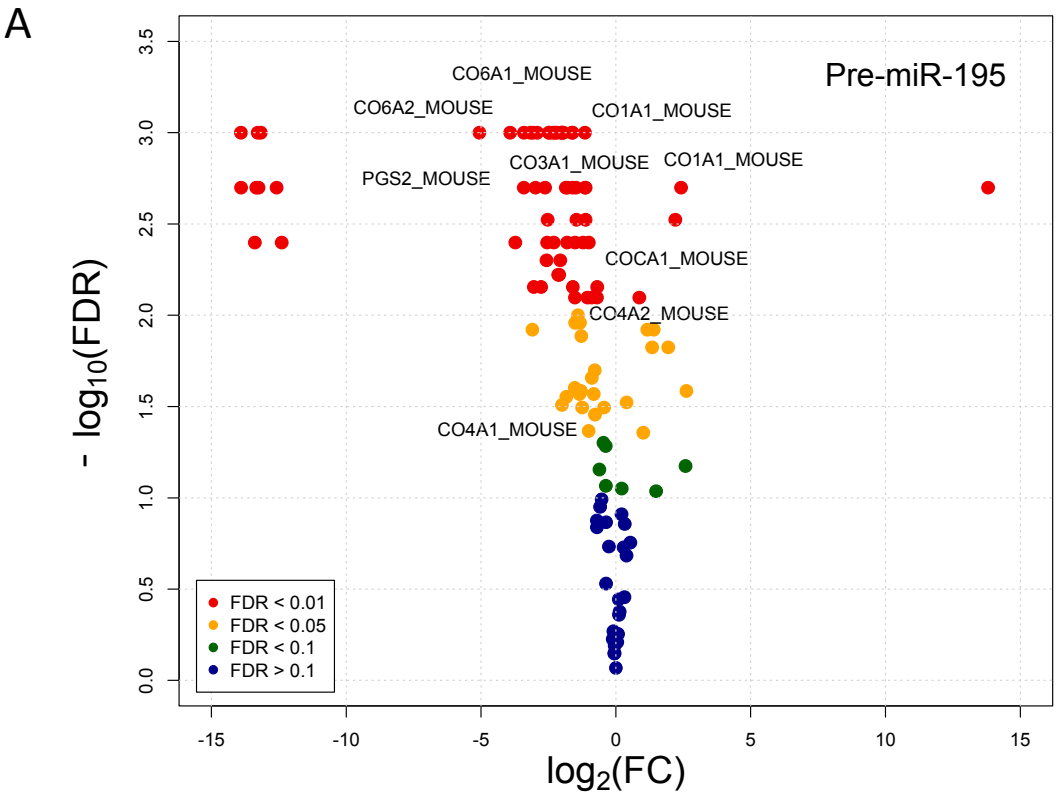
A
Pre-miR-195
CO6A1_MOUSE
CO6A2_MOUSE
CO1A1_MOUSE
CO3A1_MOUSE
CO1A1_MOUSE
PGS2_MOUSE
COCA1_MOUSE
CO4A2_MOUSE
CO4A1_MOUSE
FDR < 0.01
FDR < 0.05
FDR < 0.1
FDR > 0.1
- log10(FDR)
log2(FC)
0.0
0.5
1.0
1.5
2.0
2.5
3.0
3.5
-15
-10
-5
0
5
10
15

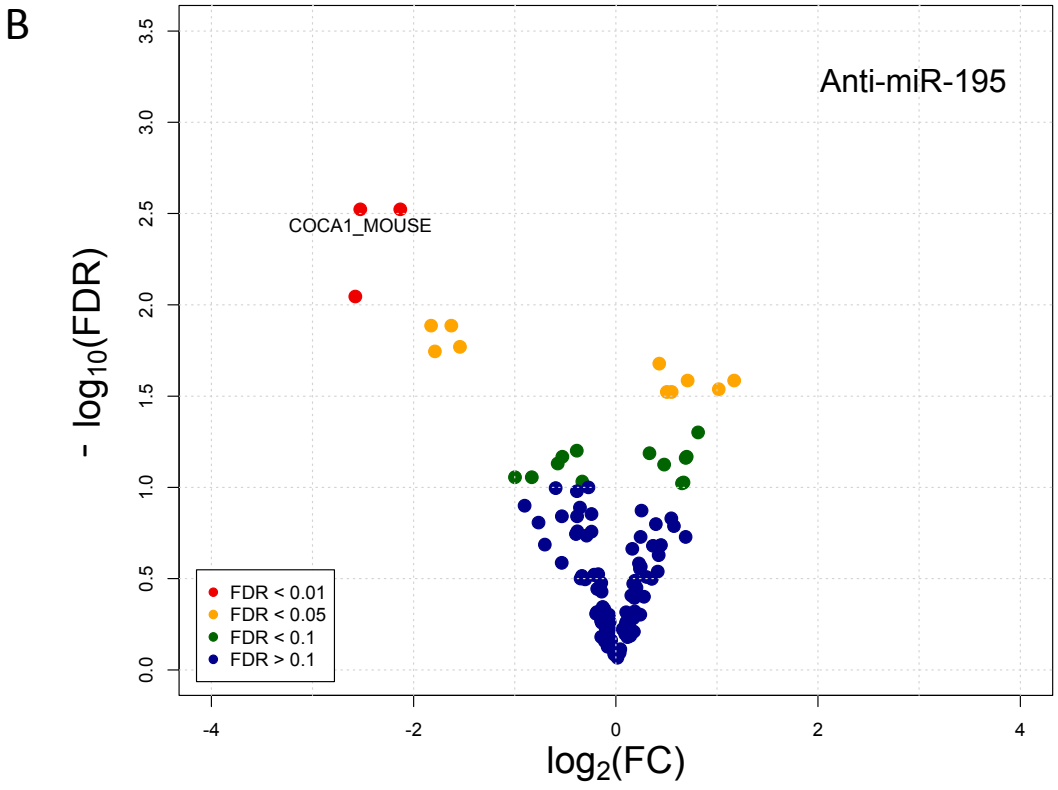
B
Anti-miR-195
COCA1_MOUSE
FDR < 0.01
FDR < 0.05
FDR < 0.1
FDR > 0.1
- log10(FDR)
log2(FC)
0.0
0.5
1.0
1.5
2.0
2.5
3.0
3.5
-4
-2
0
2
4

Figure 2

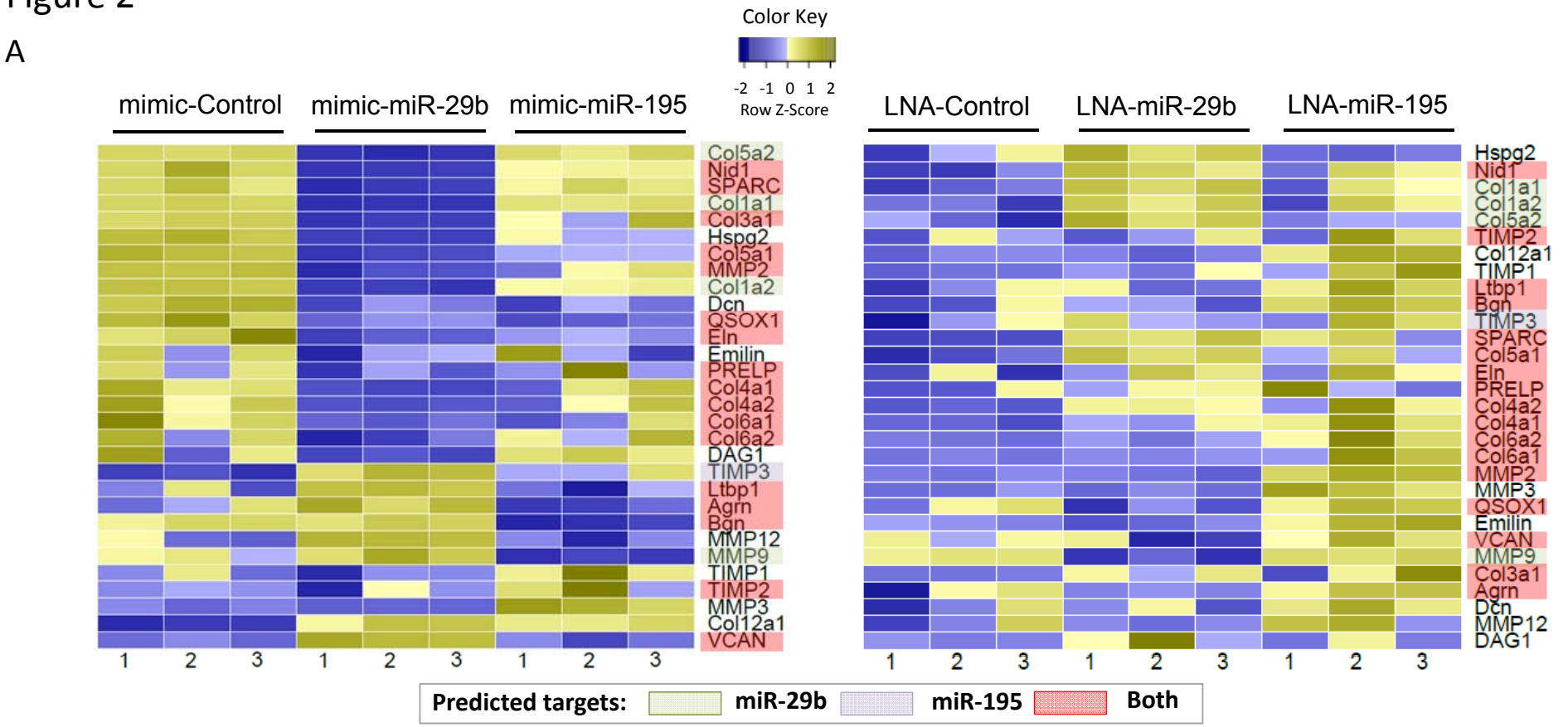
A
Color Key
-2 -1 0 1 2
Row Z-Score
mimic-Control
mimic-miR-29b
mimic-miR-195
LNA-Control
LNA-miR-29b
LNA-miR-195
Col5a2
Nid1
SPARC
Col1a1
Col3a1
Hspg2
Col5a1
MMP2
Col1a2
Dcn
QSOX1
Eln
Emilin
PRELP
Col4a1
Col4a2
Col6a1
Col6a2
DAG1
TIMP3
Ltbp1
Agrn
Bgn
MMP12
MMP9
TIMP1
TIMP2
MMP3
Col12a1
VCAN
Hspg2
Nid1
Col1a1
Col1a2
Col5a2
TIMP2
Col12a1
TIMP1
Ltbp1
Bgn
TIMP3
SPARC
Col5a1
Eln
PRELP
Col4a2
Col4a1
Col6a2
Col6a1
MMP2
MMP3
QSOX1
Emilin
VCAN
MMP9
Col3a1
Agrn
Dcn
MMP12
DAG1
1 2 3 1 2 3 1 2 3
1 2 3 1 2 3 1 2 3
Predicted targets:
miR-29b
miR-195
Both

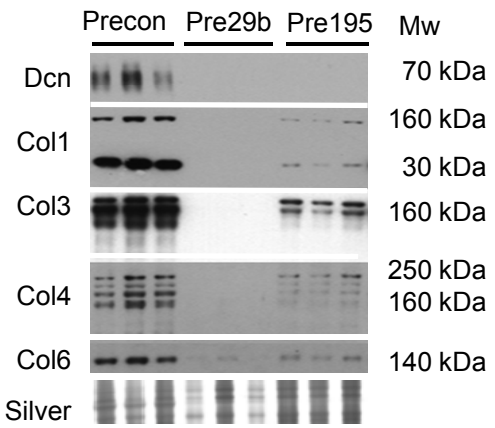
B
Precon
Pre29b
Pre195
Mw
Dcn
70 kDa
Col1
160 kDa
30 kDa
Col3
160 kDa
Col4
250 kDa
160 kDa
Col6
140 kDa
Silver

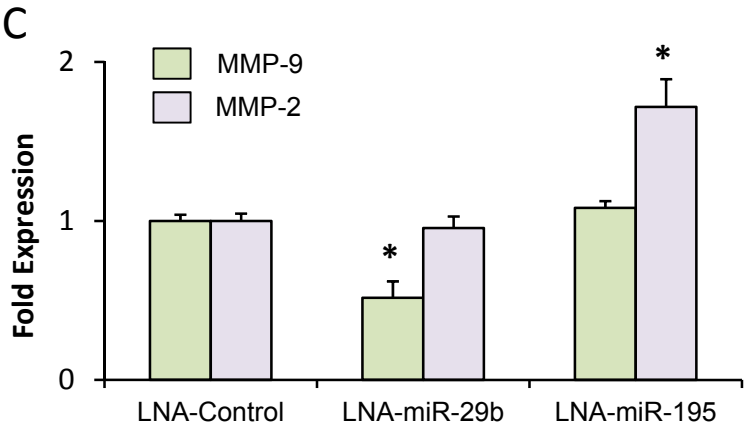
C
MMP-9
MMP-2
Fold Expression
2
1
0
*
*
LNA-Control
LNA-miR-29b
LNA-miR-195

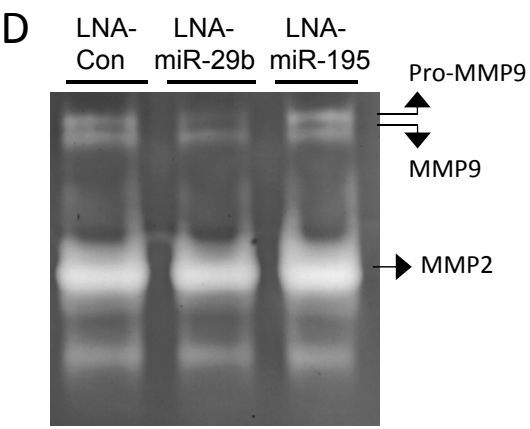
D
LNA-Con
LNA-miR-29b
LNA-miR-195
Pro-MMP9
MMP9
MMP2

Figure 3

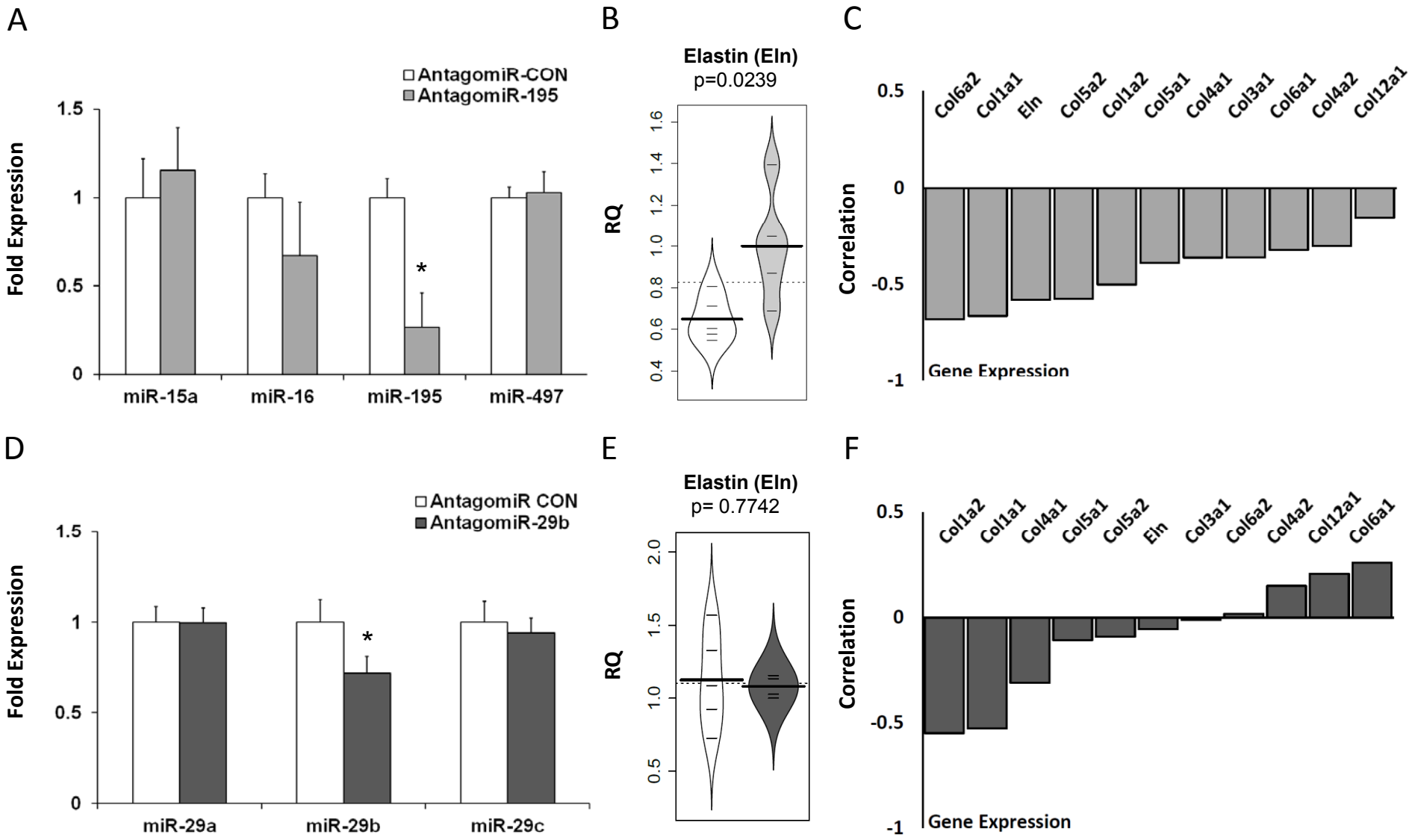
A
AntagomiR-CON
AntagomiR-195
Fold Expression
1.5
1
0.5
0
*
miR-15a
miR-16
miR-195
miR-497
B
Elastin (Eln)
p=0.0239
RQ
1.6
1.4
1.2
1.0
0.8
0.6
0.4
C
Correlation
0.5
0
-0.5
-1
Col6a2
Col1a1
Eln
Col5a2
Col1a2
Col5a1
Col4a1
Col3a1
Col6a1
Col4a2
Col12a1
Gene Expression
D
AntagomiR CON
AntagomiR-29b
Fold Expression
1.5
1
0.5
0
*
miR-29a
miR-29b
miR-29c
E
Elastin (Eln)
p= 0.7742
RQ
2.0
1.5
1.0
0.5
F
Correlation
0.5
0
-0.5
-1
Col1a2
Col1a1
Col4a1
Col5a1
Col5a2
Eln
Col3a1
Col6a2
Col4a2
Col12a1
Col6a1
Gene Expression

Figure 4

A

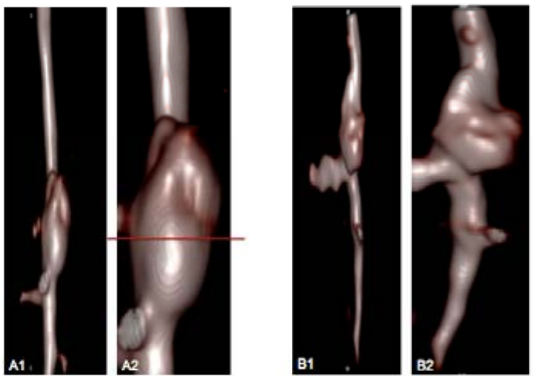

B

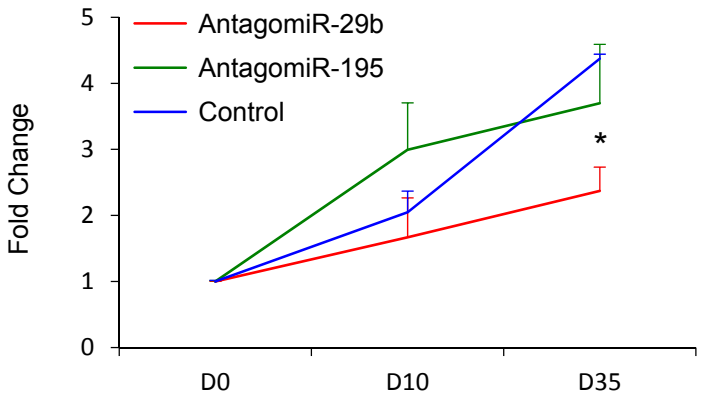

C

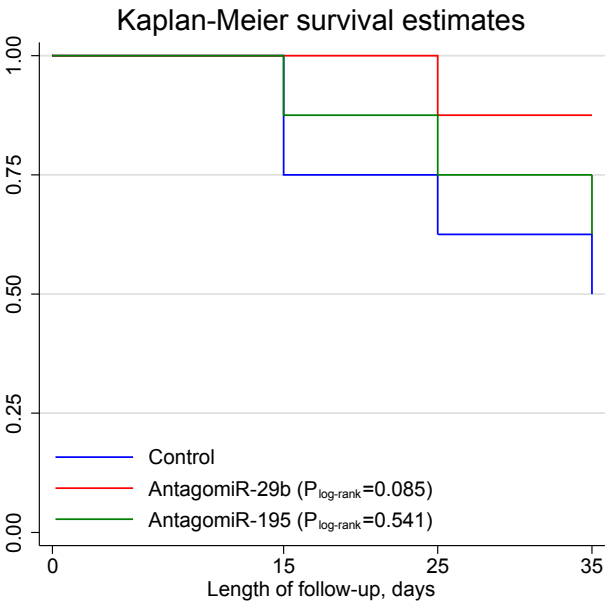

Number at risk				
Group = Control	16	16	12	10
Group = AntagomiR-29b	8	8	8	7
Group = AntagomiR-195	8	8	7	6

Figure 5

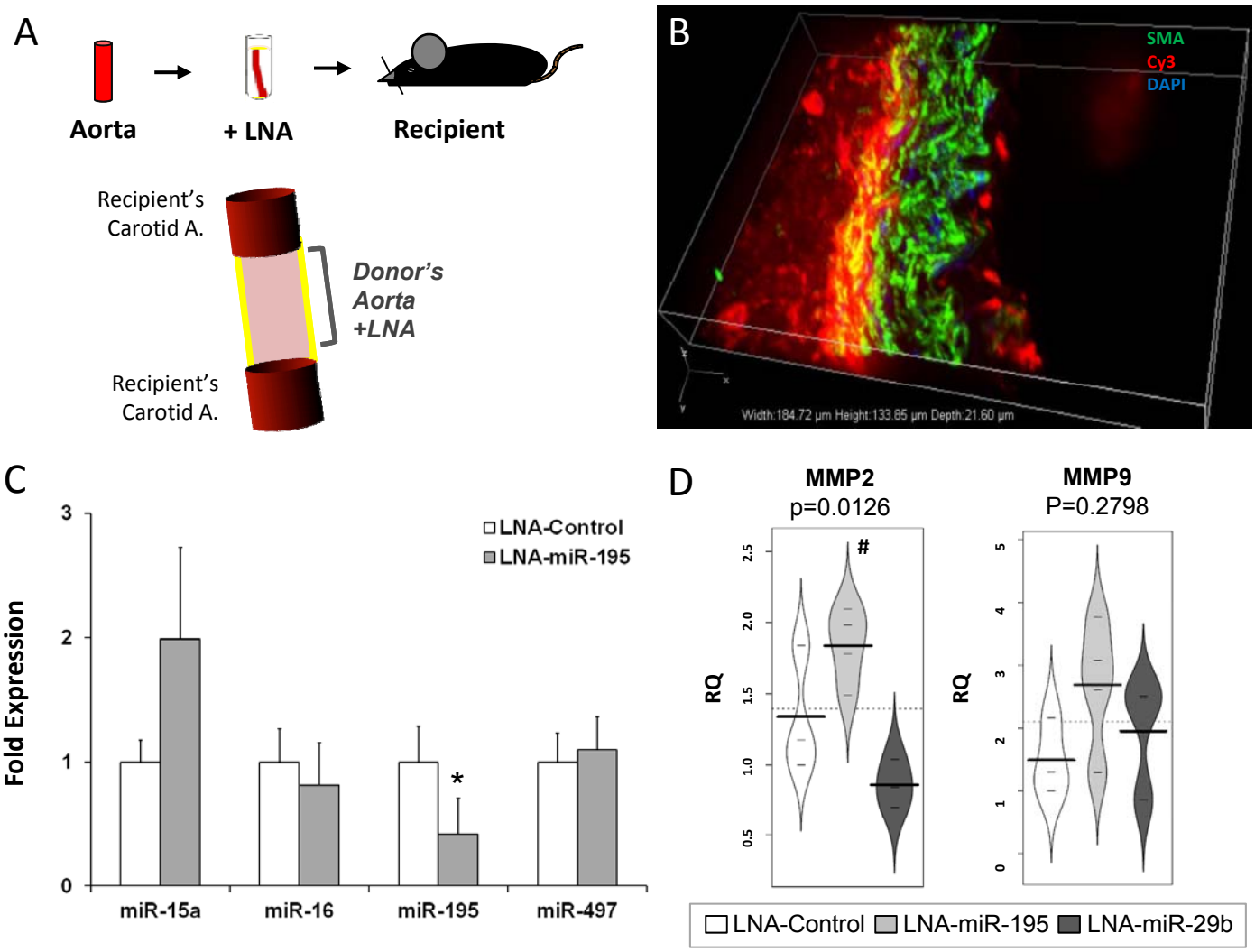

E

	n	Pearson correlation coefficient (95% CI) between log miR-195 and MMPs	P value
MMP2			
Uninjured aorta	10	-0.68 (-0.92, -0.08)	0.030
Aortic grafts	10	-0.44 (-0.84, 0.26)	0.210
Ang II day 16	8	-0.69 (-0.94, 0.03)	0.059
Overall	28	-0.60 (-0.82, -0.24)	0.002
MMP9			
Uninjured aorta	10	-0.77 (-0.94, -0.28)	0.007
Aortic grafts	10	-0.53 (-0.87, 0.14)	0.115
Ang II day 16	8	-0.78 (-0.96, -0.17)	0.020
Overall	28	-0.70 (-0.87, -0.40)	<0.001

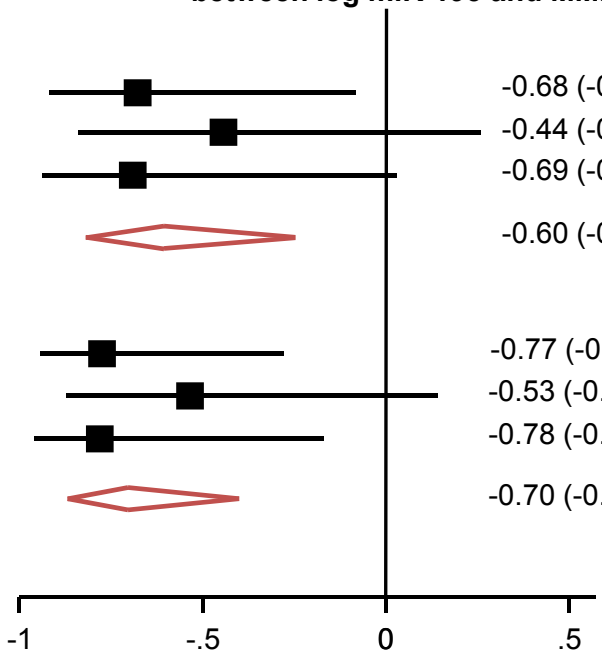

Figure 6

A

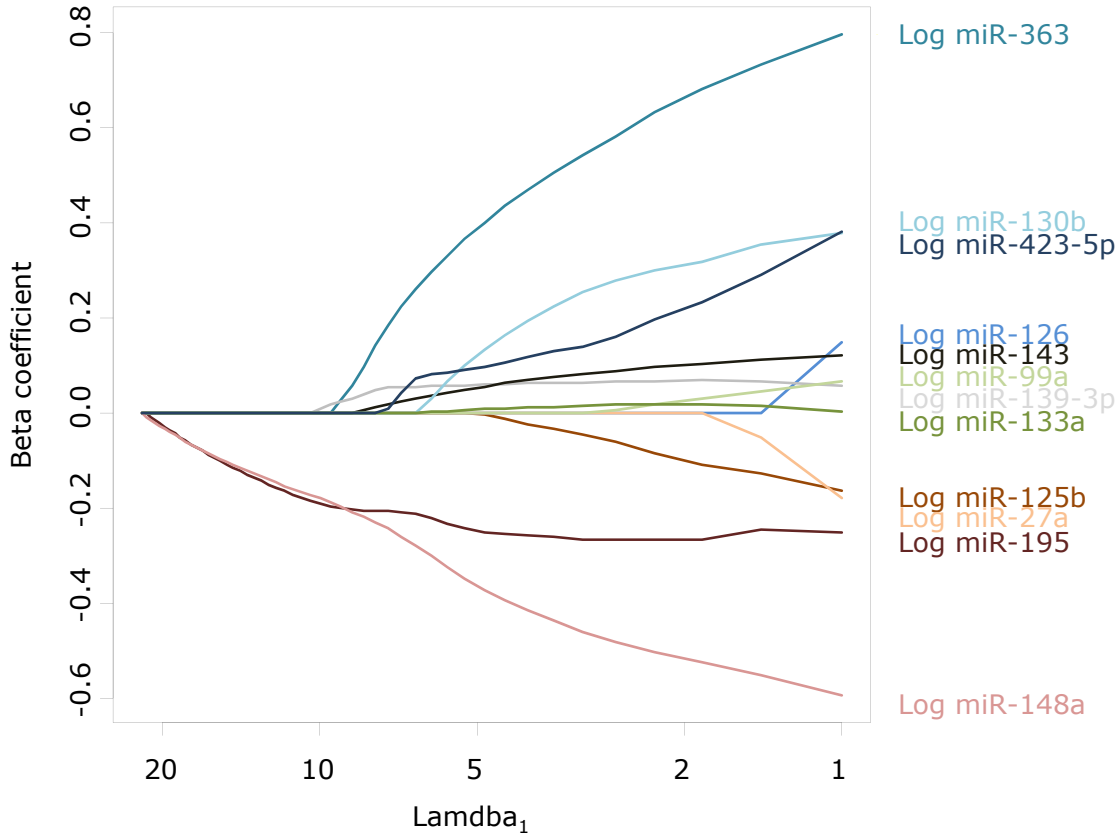
Beta coefficient
0.8
0.6
0.4
0.2
0.0
-0.2
-0.4
-0.6
20
10
5
2
1
Lamdba1
Log miR-363
Log miR-130b
Log miR-423-5p
Log miR-126
Log miR-143
Log miR-99a
Log miR-139-3p
Log miR-133a
Log miR-125b
Log miR-27a
Log miR-195
Log miR-148a

B

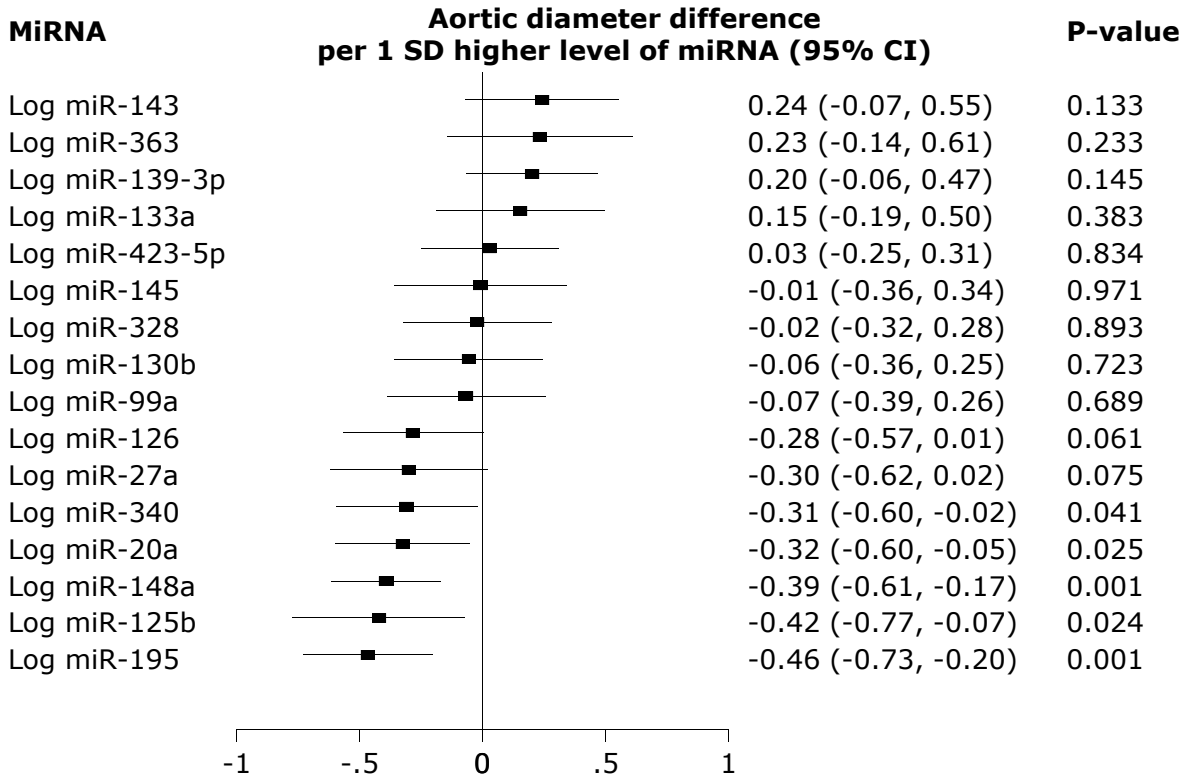
MiRNA
Aortic diameter difference per 1 SD higher level of miRNA (95% CI)
P-value
Log miR-143 0.24 (-0.07, 0.55) 0.133
Log miR-363 0.23 (-0.14, 0.61) 0.233
Log miR-139-3p 0.20 (-0.06, 0.47) 0.145
Log miR-133a 0.15 (-0.19, 0.50) 0.383
Log miR-423-5p 0.03 (-0.25, 0.31) 0.834
Log miR-145 -0.01 (-0.36, 0.34) 0.971
Log miR-328 -0.02 (-0.32, 0.28) 0.893
Log miR-130b -0.06 (-0.36, 0.25) 0.723
Log miR-99a -0.07 (-0.39, 0.26) 0.689
Log miR-126 -0.28 (-0.57, 0.01) 0.061
Log miR-27a -0.30 (-0.62, 0.02) 0.075
Log miR-340 -0.31 (-0.60, -0.02) 0.041
Log miR-20a -0.32 (-0.60, -0.05) 0.025
Log miR-148a -0.39 (-0.61, -0.17) 0.001
Log miR-125b -0.42 (-0.77, -0.07) 0.024
Log miR-195 -0.46 (-0.73, -0.20) 0.001
-1
-.5
0
.5
1

Figure 7

A

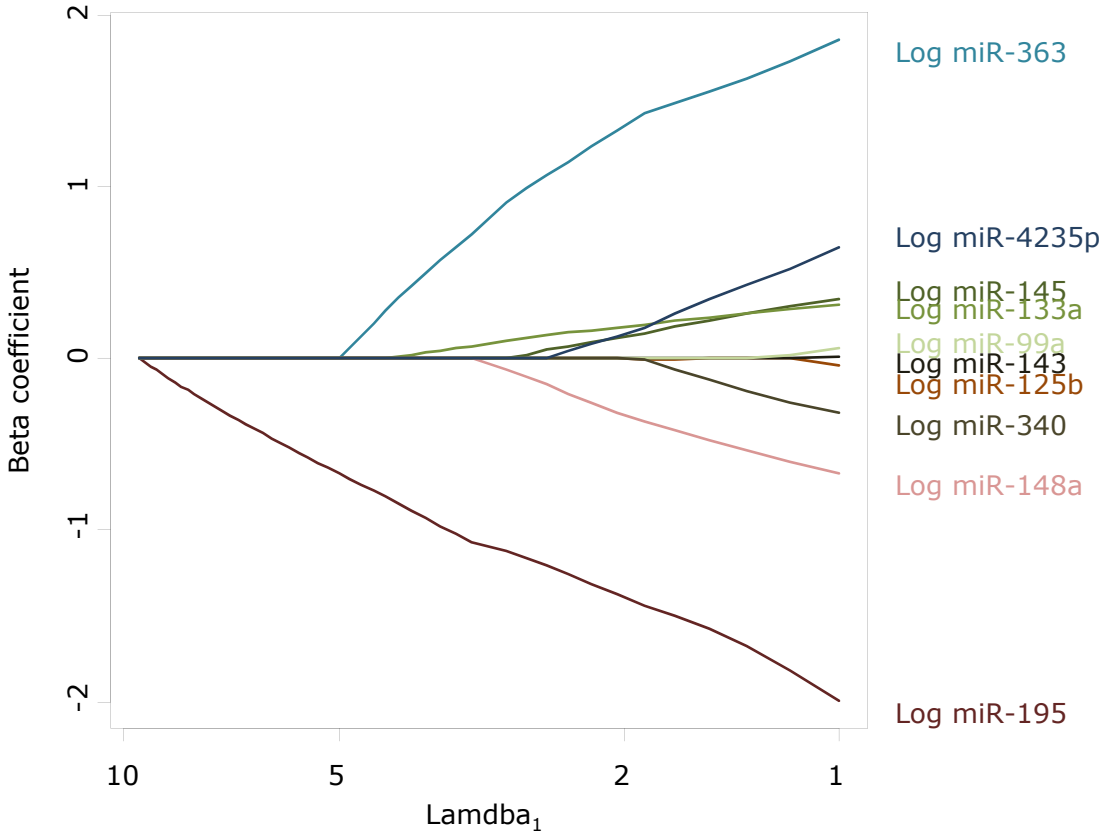
Beta coefficient
2
1
0
-1
-2
10
5
2
1
Lamdba1
Log miR-363
Log miR-4235p
Log miR-145
Log miR-133a
Log miR-99a
Log miR-143
Log miR-125b
Log miR-340
Log miR-148a
Log miR-195

B

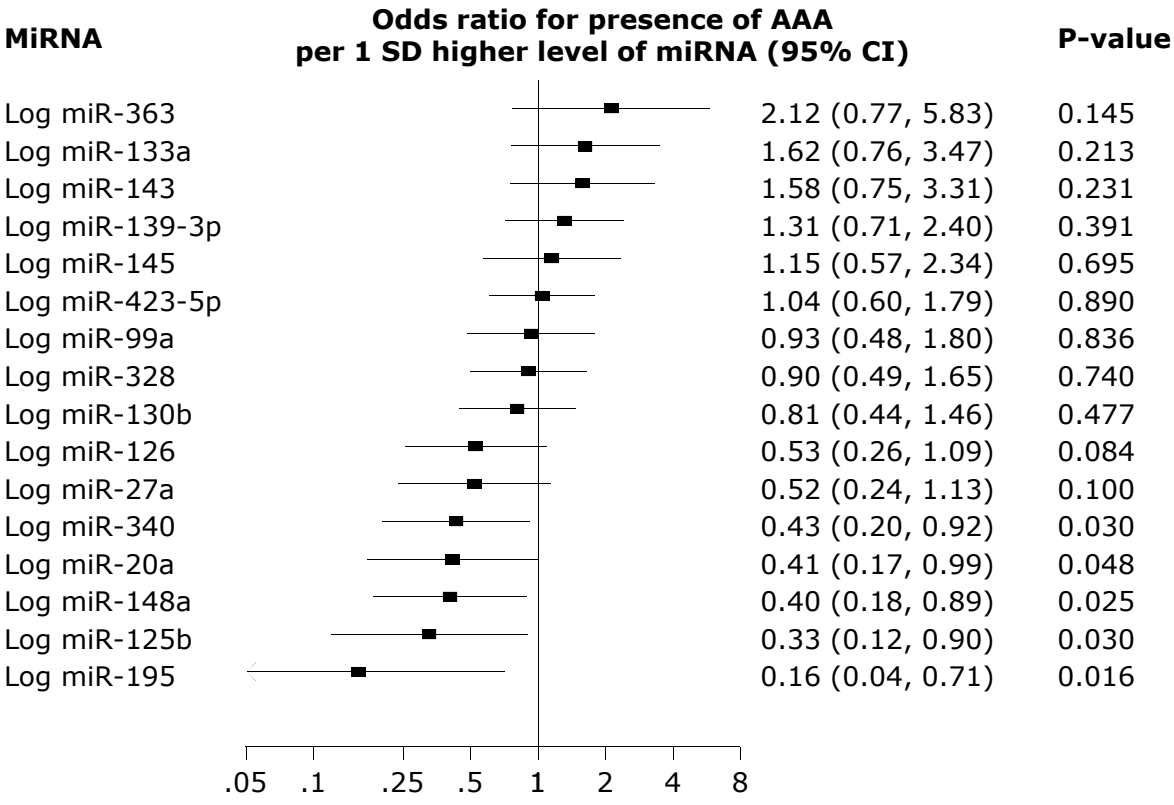
MiRNA
Odds ratio for presence of AAA per 1 SD higher level of miRNA (95% CI)
P-value
Log miR-363 2.12 (0.77, 5.83) 0.145
Log miR-133a 1.62 (0.76, 3.47) 0.213
Log miR-143 1.58 (0.75, 3.31) 0.231
Log miR-139-3p 1.31 (0.71, 2.40) 0.391
Log miR-145 1.15 (0.57, 2.34) 0.695
Log miR-423-5p 1.04 (0.60, 1.79) 0.890
Log miR-99a 0.93 (0.48, 1.80) 0.836
Log miR-328 0.90 (0.49, 1.65) 0.740
Log miR-130b 0.81 (0.44, 1.46) 0.477
Log miR-126 0.53 (0.26, 1.09) 0.084
Log miR-27a 0.52 (0.24, 1.13) 0.100
Log miR-340 0.43 (0.20, 0.92) 0.030
Log miR-20a 0.41 (0.17, 0.99) 0.048
Log miR-148a 0.40 (0.18, 0.89) 0.025
Log miR-125b 0.33 (0.12, 0.90) 0.030
Log miR-195 0.16 (0.04, 0.71) 0.016
.05
.1
.25
.5
1
2
4
8